Rapidity Gap Events at HERA and the Structure of the Pomeron

Julian P. Phillips

Oliver Lodge Laboratory, The University of Liverpool, England

representing the H1 and ZEUS collaborations

Abstract

Recent measurements, using data taken with the H1 and ZEUS detectors at the HERA ep collider, of the cross sections for processes involving large rapidity gaps in the observed final states are presented. Measurements of the contribution, $F_2^{D(3)}$, of these events to the proton structure function establish for the first time that they are of a dominantly diffractive origin. A QCD analysis of the deep–inelastic structure of $F_2^{D(3)}$and measurements of jet production in photoproduction interactions suggests that the rôle of gluons in these diffractive interactions is significant.

1. Introduction

The rise with increasing centre of mass energy of total hadron–hadron cross sections may be accurately parameterised within the Regge framework, where the high energy behaviour is attributed to the soft pomeron ($I\!P$) trajectory, $\alpha_{I\!P}(t) = 1.08 + \alpha'_{I\!P}t$ [1]. However, no microscopic understanding of this mechanism in terms of QCD theory is established. Furthermore, measurements at HERA of the deep–inelastic structure of the proton at low Bjorken–x are incompatible with the expectations of the soft pomeron. Recent data taken at HERA, featuring the production of spectacular "rapidity gaps" in the final state, offer a singular opportunity to investigate the structure of diffractive exchange, that is of the $I\!P$. In this paper, the first measurements of the diffractive contribution to the proton structure function, $F_2^{D(3)}$, are reviewed along with measurements of jet production in photoproduction interactions. Possible partonic interpretations of the structure revealed are discussed, and the first indications that gluons play a dominant rôle in diffractive ep collisions outlined.

2. Measurement of $F_2^{D(3)}$at HERA

The data were taken with the H1 and ZEUS detectors at the HERA ep collider in 1993, in which 26.7 GeV electrons were in head–on collision with 820 GeV protons. The data analysed by the H1 and ZEUS collaborations correspond to integrated luminosities of $272 \pm 14\,\mathrm{nb}^{-1}$ and $540 \pm 18\,\mathrm{nb}^{-1}$ respectively.

In the following, a coordinate system is used with origin at the interaction point and z axis along the proton beam, or forward, direction. The pseudo–rapidity of a final state particle with polar angle θ in the laboratory is then $\eta = -\ln\tan\frac{\theta}{2}$.

From samples of deep–inelastic scattering data ($Q^2 \gtrsim 4\,\mathrm{GeV}^2$), large rapidity gap events were selected. The selection of such events, in which there is no energy flow adjacent to the direction of any proton remnant, requires detectors with the best possible coverage in the forward region.

The selection of H1 used the main liquid argon (LAr) calorimeter ($-1.51 < \eta < 3.65$) along with detectors in the forward region. Due to secondary interactions of hadrons with the collimators, the beam–pipe and adjunct material, the forward muon detector (FMD) and forward "plug" calorimeter (PLUG) are sensitive to the production of hadrons in the pseudo–rapidity ranges $3.54 < \eta < 5.08$ and $5.0 < \eta < 6.6$ respectively. By demanding no energy deposition above a threshold of 400 MeV in the LAr in the region $\eta > 3.2$, along with no activity above thresholds in the PLUG or FMD, events exhibiting a rapidity gap of at least 3.4 units of pseudo–rapidity extending towards the central region from the forward acceptance limit of $\eta = 6.6$ were selected [2].

The selection of ZEUS used information from the main uranium calorimeter. A cut is made on the "angle" of the hadronic system measured in main

* Invited talk in the session of diffraction and vector mesons in the working group I at the workshop on Deep–Inelastic Scattering, Paris, 1995.

calorimeter. This angle, θ_H, is defined by $\cos\theta_H = \sum_i p_{z_i}/\sum_i \vec{p_i}$ where $\vec{p_i}$ is the momentum vector of the calorimeter cell i, where the sum is over all cells in the calorimeter not associated with the scattered electron. Studies of Monte Carlo simulations of diffractive and non–diffractive events suggest that the former may be identified with the selection $\cos\theta_H < 0.75$. In addition, a rapidity gap of at least 1.8 units in pseudorapidity starting at the forward limit of the acceptance, $\eta = 4.3$, is required [3].

The measurements of $F_2^{D(3)}$ presented here are made as a function of the three kinematic variables x, Q^2, and $x_{I\!P}$, or equivalently β, Q^2, and $x_{I\!P}$. They are defined as follows:

$$x = \frac{-q^2}{2P \cdot q} \qquad x_{I\!P} = \frac{q \cdot (P - P')}{q \cdot P} \tag{1}$$

$$Q^2 = -q^2 \qquad \beta = \frac{-q^2}{2q \cdot (P - P')}. \tag{2}$$

Here q, P and P' are the 4–momenta of the virtual boson, the incident proton, and the final state colourless remnant respectively. Note that $x = \beta x_{I\!P}$. It is convenient to write $x_{I\!P}$ and β above as

$$x_{I\!P} = \frac{Q^2 + M_X^2 - t}{Q^2 + W^2 - M_p^2} \approx \frac{Q^2 + M_X^2}{Q^2} \cdot x = x_{I\!P/p} \tag{3}$$

$$\beta = \frac{Q^2}{Q^2 + M_X^2 - t} \approx \frac{Q^2}{Q^2 + M_X^2} = x_{q/I\!P} \tag{4}$$

where M_X is the invariant mass of the hadronic system excluding the colourless remnant, $t = (P - P')^2$ is the 4–momentum transfer squared at the incident proton vertex, and W is the total hadronic invariant mass. In the kinematic domain of these measurements $x_{I\!P}$ may be interpreted as the fraction $x_{I\!P/p}$ of the 4–momentum of the proton carried by the diffractive exchange, that is the interacting $I\!P$ if such a picture is invoked, and β as the fraction $x_{q/I\!P}$ of the 4–momenta of the $I\!P$ carried by the quark interacting with the virtual boson.

A structure function $F_2^{D(4)}$ is defined [2] by analogy with the decomposition of the unpolarised total ep cross section. It is written in terms of two structure functions $F_2^{D(4)}$ and $\frac{F_2^{D(4)}}{2x(1+R^{D(4)})}$ in the form (α is here the fine structure constant)

$$\frac{\mathrm{d}^4\sigma_{ep\to epX}}{\mathrm{d}x\mathrm{d}Q^2\mathrm{d}x_{I\!P}\,dt} = \frac{4\pi\alpha^2}{xQ^4}\left\{1 - y + \frac{y^2}{2[1+R^{D(4)}]}\right\} \cdot F_2^{D(4)}(x, Q^2, x_{I\!P}, t) \tag{5}$$

in which y is the usual DIS scaling variable given by $y = Q^2/sx$. s is the ep collision centre of mass (CM) energy squared. In these measurements the selected data are predominantly at low y so that there is little sensitivity to $R^{D(4)}$. The measurements used data in which the final state colourless remnant was not detected. Therefore no accurate determination of t was possible and the measured cross sections amounts to $\frac{d^3\sigma(ep\to epX)}{\mathrm{d}x\mathrm{d}Q^2\mathrm{d}x_{I\!P}}$, from which it is possible to determine only $F_2^{D(3)}(x, Q^2, x_{I\!P}) = \int F_2^{D(4)}(x, Q^2, x_{I\!P}, t)\,\mathrm{d}t$ provided that a particular choice is made for $R^{D(4)}$ and its t dependence. For these measurements, $R^{D(4)}$ was set to 0 and $F_2^{D(3)}$ was evaluated from

$$\frac{\mathrm{d}^3\sigma_{ep\to epX}}{\mathrm{d}x\mathrm{d}Q^2\mathrm{d}x_{I\!P}} = \frac{4\pi\alpha^2}{xQ^4}\left\{1 - y + \frac{y^2}{2}\right\} F_2^{D(3)}(x, Q^2, x_{I\!P}) \tag{6}$$

following the original procedure of [5].

Both collaborations used Monte Carlo simulations of deep–inelastic electron–pomeron (e–$I\!P$) scattering and of low mass vector meson production for the determination of acceptances and experimental biases. In addition, standard simulations which did not explicitly include diffractive interactions were used to determine the backgrounds from non–diffractive processes [2, 3, 4, 16].

The measurements of $F_2^{D(3)}$by both collaborations contain a contribution from interactions in which the scattered proton dissociates (proton inelastic). H1 have corrected $F_2^{D(3)}$to the total contribution from both proton elastic and proton inelastic processes. ZEUS have produced a measurement in which the contribution from proton inelastic processes which remain in the selected sample is estimated. In order to make an absolute comparison of the two measurements, here each is corrected in overall normalisation to the proton elastic cross section, and the $(\beta, Q^2, x_{I\!P})$ dependence of the two structure functions, corrected in this way, are shown in figure 1.

3. Factorisation of $F_2^{D(3)}$and Evidence for Diffraction

Everywhere $F_2^{D(3)}$ is observed to decrease monotonically with increasing $x_{I\!P}$ in the measured ranges. Both collaborations obtain an excellent fit to all data points, irrespective of β and Q^2, assuming a dependence $x_{I\!P}^{-n}$. The result of such a fit to the H1 data is shown in figure 3. H1 obtain a value for n of $1.19 \pm 0.06(stat.) \pm 0.07(syst.)$ with $\chi^2/\mathrm{d.f.} = 32.0/46$, 94% C.L. The value of n measured by the ZEUS collaboration is $1.30 \pm 0.08(stat.)^{+0.08}_{-0.14}(syst.)$, and is consistent with that of H1. No evidence for any systematic trend in the contributions to χ^2 as a function of β and Q^2 is reported.

Such a universal dependence on $x_{I\!P}$ is expected naïvely if the deep–inelastic process responsible for rapidity gap events involves a (colourless) target $I\!P$ in the incident proton whose characteristics are not dependent on $x_{I\!P}$, and which carries only a small

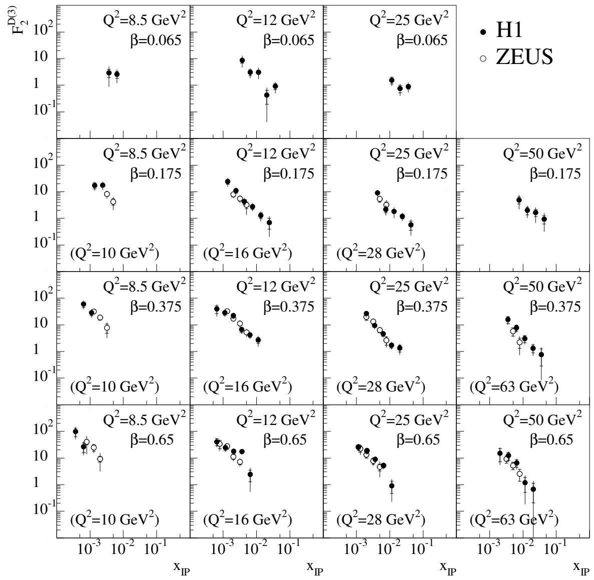

Figure 1. The proton elastic diffractive contribution $F_2^{D(3)}$ to the proton structure function F_2 as a function of $x_{I\!P}$ for different β and Q^2 values; the inner error is the statistical error; the full error shows the statistical and systematic error added in quadrature. The open circles are the ZEUS data; the closed circles are the H1 data. Where ZEUS data are available, the Q^2 values for the ZEUS data are shown in parentheses.

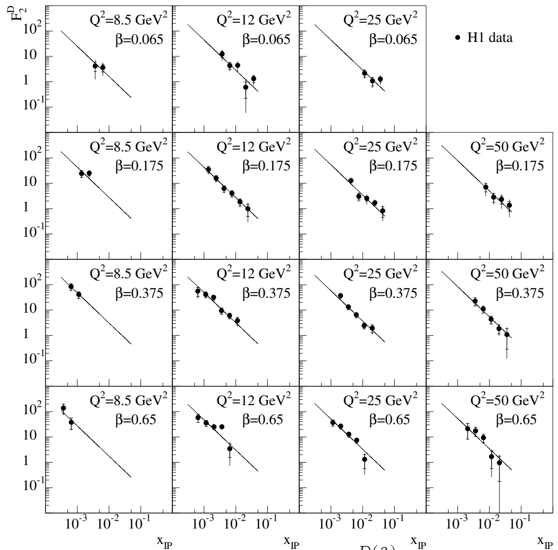

Figure 2. The H1 measurement of $F_2^{D(3)}$ as a function of $x_{I\!P}$ for different β and Q^2 values; the inner error is the statistical error; the full error shows the statistical and systematic error added in quadrature; superimposed is the result of a fit establishing a factorisable dependence of the form $\propto x_{I\!P}^{-n}$ (see text).

fraction of the proton's momentum. The dependence of $F_2^{D(3)}(\beta, Q^2, x_{I\!P})$ then factorises into the product of a universal term ($f_{I\!P/p}(x_{I\!P}) \propto x_{I\!P}^{-n}$), which describes the "flux" of $I\!P$ "in" the proton, and a term which describes any structure of $I\!P$ and which is a function of only β and Q^2. The diffractive structure function $F_2^{D(3)}$ can then be written

$$F^{D(3)}(\beta, Q^2, x_{I\!P}) = f_{I\!P/p}(x_{I\!P}) \cdot F_2^{I\!P}(\beta, Q^2) \qquad (7)$$

where $F_2^{I\!P}(\beta, Q^2)$, describes the deep–inelastic structure of the target $I\!P$ [6].

If the colourless component $I\!P$ of the proton is taken to be well parameterised as a "Reggeised" hadronic exchange, then the $x_{I\!P}$ dependence of the flux factor is specified by the leading Regge trajectory $\alpha(t)$ in the "asymptotic limit" $x_{I\!P} \to 0$, $t/s \to 0$. The dependence takes the form $x_{I\!P}^{-[2\alpha(t)-1]}$. These measurement are, however, integrated over t. If the effects of finite t and the contributions from proton inelastic interactions are neglected, then $\alpha(t)$ may be replaced by $\alpha_{t=0}$ and the observed $x_{I\!P}$ dependence corresponds to $\alpha_{t=0} = 1.10 \pm 0.03(stat.) \pm 0.04(syst.)$ for the H1 measurements and $\alpha_{t=0} = 1.15 \pm 0.04(stat.)^{+0.04}_{-0.07}(syst.)$ for the ZEUS measurement. Corrections to these values of $\alpha_{t=0}$ require further assumptions about the as yet unmeasured t dependence of the flux factor and mass distribution of the proton remnant in proton inelastic interactions, and are discussed in [6].

The measurements are therefore consistent with the leading trajectory which describes phenomenologically "soft hadronic" diffractive interactions, namely the pomeron ($I\!P$) with $\alpha(t) = \alpha_{I\!P}(0) + \alpha' t$ and $\alpha_{I\!P}(0) = 1.085$, $\alpha' = 0.25\,\mathrm{GeV}^{-2}$ [6]. This does not rule out a "hard" (BFKL) $I\!P$ ($\alpha_{I\!P}(0) \lesssim 1.5$ [7, 8]) particularly if it contributes together with a soft component, such as that described above. A recent calculation, based on a BFKL approach, suggests also that the simplest factorisation with an $x_{I\!P}$ dependence $\propto x_{I\!P}^{-n}$ may not strictly hold [9]. The accuracy of this measurement of the $x_{I\!P}$ dependence does not exclude such a possibility.

Note that the intercepts for the leading meson Regge trajectories and any parameterisation of pion exchange give rise to an $x_{I\!P}$ dependence which is much less steep. Therefore the interpretation of the rapidity gap events in DIS at low Bjorken–x as being due to diffraction can be made without ambiguity.

4. The Partonic Structure of Proton Diffraction

4.1. QCD Analysis of the Deep–Inelastic Structure of Proton Diffraction

The observation that the rapidity gap events are of a predominantly diffractive nature, and the evidence for simple factorisation of the diffractive dependence on $x_{I\!P}$ lead naturally to the interpretation of the β and Q^2 dependencies of $F_2^{D(3)}$ as a measure of the deep–inelastic structure of diffractive exchange.

In figure 3 are shown the β and Q^2 dependencies of the integral

$$\tilde{F}_2^D(\beta, Q^2) = \int_{x_{\mathbb{P}_L}}^{x_{\mathbb{P}_H}} F_2^{D(3)}(\beta, Q^2, x_{\mathbb{P}})\, \mathrm{d}x_{\mathbb{P}}, \quad (8)$$

which, assuming factorisation of the diffractive dependence on $x_{\mathbb{P}}$, is proportional to the structure function of the $\mathbb{P}$. The range of integration, $x_{\mathbb{P}_L} = 3 \times 10^{-4}$ to

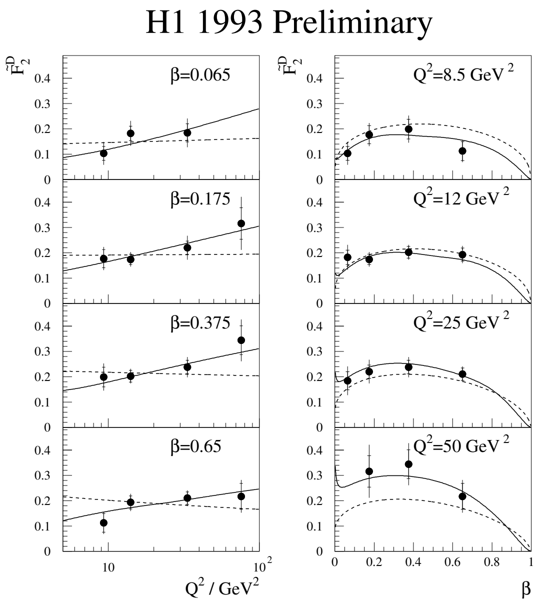

Figure 3. Dependence of $\tilde{F}_2^D$ on Q^2 and β; superimposed are the results of two LO $\log Q^2$ DGLAP QCD fits. The dashed line shows a fit in which at the starting scale, $Q_0^2 = 4\,\mathrm{GeV}^2$, diffraction is attributed to the exchange of only quarks (χ^2/dof of 13/12, 37%C.L.). The solid line shows a fit in which both quarks and gluons may contribute to the diffractive mechanism at $Q_0^2 = 4\,\mathrm{GeV}^2$ (χ^2/dof = 4/9, 91%C.L.). In the latter, the gluons carry $\sim 90\%$ of the momentum of the pomeron at $Q_0^2 = 4\,\mathrm{GeV}^2$. The data are those published in [2].

$x_{\mathbb{P}_H} = 0.05$, is chosen to span the entire $x_{\mathbb{P}}$ range of measurement of $F_2^{D(3)}$. It is convenient to extract the dependence of $F_2^{D(3)}$on β and Q^2 in this way in order to avoid the need to specify the theoretically ill–defined normalisation of the diffractive flux. In a factorisable interpretation of diffraction, then for a particular choice of the pomeron flux, $\tilde{F}_2^D(\beta, Q^2)$ may be related to the structure function of the pomeron $F_2^{\mathbb{P}}$:

$$\tilde{F}_2^D(\beta, Q^2) = F_2^{\mathbb{P}}(\beta, Q^2) \cdot \int_{x_{\mathbb{P}_L}}^{x_{\mathbb{P}_H}} f_{\mathbb{P}/p}(x_{\mathbb{P}})\mathrm{d}x_{\mathbb{P}}. \quad (9)$$

There is no evidence for any substantial Q^2 dependence of $\tilde{F}_2^D$ for any β. Deep (high Q^2) diffractive interactions are thus broadly of a scale invariant, and therefore point-like, nature. Furthermore, $\tilde{F}_2^D$ is observed to have little dependence on β with contributions throughout the measured range. Therefore the structure which is resolved by the electron in the high Q^2 diffractive interaction carries only a fraction of the $\mathbb{P}$'s momentum, implying that the $\mathbb{P}$ has its own point-like partonic sub–structure. A similar treatment of the ZEUS measurement of $F_2^{D(3)}$confirms these conclusions [3].

A fit to the hypothesis of a linear $\log_{10} Q^2$ dependence of the form

$$\tilde{F}_2^D(\beta, Q^2) = a(\beta)\log_{10}Q^2 + b(\beta) \quad (10)$$

yields values for $a(\beta)$ that are $\simeq 1.5\sigma$ above zero for all values of β. The lack of any fall of $\tilde{F}_2^D$ with increasing Q^2 at large β contrasts with the violations of scale invariance exhibited by the structure function of a typical hadron. For example, the proton structure function F_2 rises with increasing Q^2 for $x \lesssim 0.15$, and falls with increasing Q^2 for $x \gtrsim 0.15$. This decreasing dependence at high x is an inevitable consequence of DGLAP QCD evolution for an object with a structure built from the evolution of "valence" quarks in which the latter predominate at large Bjorken–x. By analogy, a structure function for which any violation of scale invariance amounts to an increase with $\log Q^2$ at high Bjorken–x (β), is likely to have a large gluon, relative to quark, parton density.

To quantify any substantive evidence for a gluonic contribution to $\tilde{F}_2^D$, the DGLAP evolution equations were solved numerically in the LO and in the next–to–leading order (NLO) $\log Q^2$ approximations. Starting from a scale $Q_0^2 = 4\,\mathrm{GeV}^2$, assumed forms for the gluon and singlet quark parton densities in diffractive exchange were evolved to higher Q^2 and compared with the measurements of the β dependence of $\tilde{F}_2^D$. The parton densities which specify the structure of diffractive exchange were expressed as functions of z, the momentum of the parton as a fraction of the momentum carried in the exchange, that is of the $\mathbb{P}$ ($z = x_{i/\mathbb{P}}$, quark $i = q$, gluon $i = g$). The basic kinematic features of the method, for example the treatment of charm, were identical to those in the QCD analysis of the proton structure function F_2 [10]. However, no momentum sum rule was imposed because it is far from clear whether one should exist for such a space–like exchange, and because the normalisation of $\tilde{F}_2^D$ does not coincide with the normalisation of the structure function of diffractive exchange without further theoretical input.

The assumption that diffractive exchange contains only a flavour singlet quark density of the form $zq(z) = A_q \cdot z(1-z)$ at $Q_0^2 = 4\,\mathrm{GeV}^2$ resulted in a description of $\tilde{F}_2^D$ in LO with a χ^2/dof of 22/14 (7%C.L.). Allowing a more flexible form for the singlet quark distribution of $zq(z) = A_q \cdot z^{B_q}(1-z)^{C_q}$ yielded an acceptable solution with a χ^2/dof of 13/12 (37%C.L.) and with a flatter distribution function $B_q \sim 0.35$ and $C_q \sim 0.35$. The result of this fit is shown in figure 3 as the dashed curve. Though numerically acceptable, such a "valence" quark based solution results in a decrease of $F_2^{D(3)}$with increasing $\log Q^2$ at high β as is to be expected following the discussion above, a trend which is not favoured by the measurements of $\tilde{F}_2^D$.

The addition of a gluon density of the form $zg(z) = A_g \cdot z^{B_g}(1-z)^{C_g}$ at $Q_0^2 = 4\,\mathrm{GeV}^2$ to the singlet quark density resulted in an excellent description of $\tilde{F}_2^D(\beta, Q^2)$ ($\chi^2/\mathrm{dof} = 4/9$, 91%C.L.) which reproduces the rise with $\log Q^2$ at higher β. In this solution, shown by the solid curve in figure 3, at $Q_0^2 = 4\,\mathrm{GeV}^2$ the gluons carry $\sim$ 90% of the momentum of diffractive exchange, and the fitted gluon density is very hard, tending to $z = 1$, indicating that the structure of diffraction may involve the leading exchange of a single gluon (figure 4).

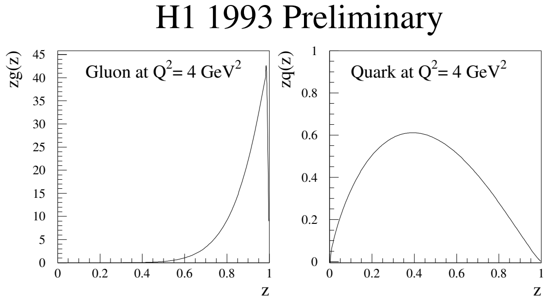

Figure 4. The quark flavour–singlet $zq(z)$ and the gluon $zg(z)$ densities at the starting scale $Q_0^2 = 4\,\mathrm{GeV}^2$ in the LO QCD description of $\tilde{F}_2^D$ which describes the well the tendency for a rise with increasing $\log Q^2$ at high β by means of a leading gluon density.

Since the evidence for a rise of $\tilde{F}_2^D$ with $\log Q^2$ at high β is of marginal significance and amounts to no more than evidence against a falling $\log Q^2$ dependence, the gluon density which is necessary to reproduce the high β behaviour is not well constrained. In all cases in which a finite gluon density is included in the diffractive exchange at the starting scale $Q_0^2 = 4\,\mathrm{GeV}^2$, repeating the fits in NLO DGLAP reduces somewhat the fractional momentum carried by the gluons.

4.2. Hard Interactions in Diffractive Photoproduction

In the photoproduction regime at HERA ($Q^2 \lesssim 4\,GeV^2$), the presence of hard scattering in diffractive processes has been identified by the characteristic increase of transverse thrust with increasing transverse energy, and by the observation of jet production [11, 12]. Motivated by this, an attempt may be made to measure jet cross sections, which are expected to reflect the dynamics of the outgoing partons from the hard scattering, and so extract information about the parton distributions in the proton associated with diffractive processes, or equivalently if a factorisable model is invoked, the parton distributions of the pomeron.

The ZEUS collaboration have used a cone algorithm in (laboratory system) η–ϕ space with a cone radius of 1 unit to identify jets with large transverse energy, E_T^{jet}, in photoproduction events [13]. The data were corrected for acceptance and experimental bias using the PYTHIA [15] and POMPYT [16] programs to model non–diffractive and diffractive hard scattering processes respectively. A selection of $\eta_{max} < 1.8$, where η_{max} is the (laboratory) pseudo–rapidity of the most forward energy deposition observed, was made in order to study the production of jets in a sample of large rapidity gap events. The results for the differential cross section $d\sigma/d\eta^{jet}$ for events with $\eta_{max} < 1.8$ in the kinematic range $E_T^{jet} > 8\,\mathrm{GeV}$, $Q^2 \leq 4\,\mathrm{GeV}^2$ and $0.2 < y < 0.85$ are presented in figure 5 as a function of the pseudo–rapidity of the jet. The non–diffractive contribution

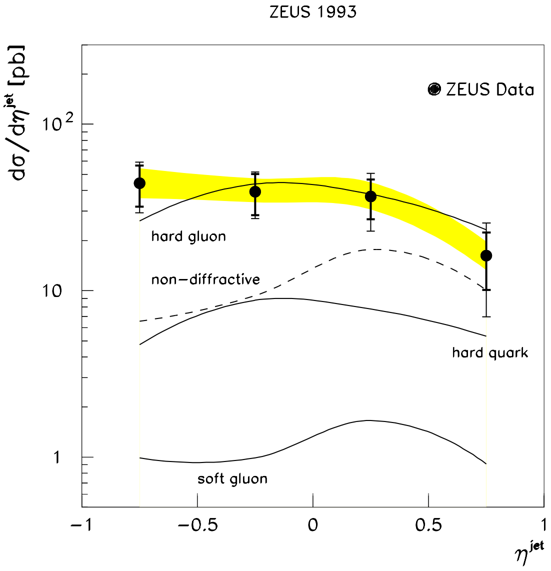

Figure 5. $d\sigma/d\eta_{jet}(\eta_{max} < 1.8)$ for inclusive jet production for $E_T^{jet} > 8\,\mathrm{GeV}$, $Q^2 < 4\,\mathrm{GeV}^2$ and $0.2 < y < 0.85$ (points). The inner error is the statistical error; the full error shows the statistical and systematic error added in quadrature. An additional error from the uncertainty of the energy scale of the calorimeter is shown as the shaded region. Also shown are the expectations from non–diffractive processes, and diffractive processes with various parton densities for the pomeron (see text).

to $d\sigma/d\eta^{jet}(\eta_{max} < 1.8)$, estimated using PYTHIA, is shown as the dashed line in figure 5. It is found to be insufficient to describe the observed rate of jet production, and this conclusion is unaffected by the particular choices made for the parton densities of the proton and of the photon.

Also shown in figure 5 are the results of calculations of the predictions of different diffractive models. A factorisable model was used such that the effective parton densities presented to the photon probe by the diffractive exchange may be represented by the product of a flux factor of pomerons “in” the proton and a set of parton densities for the pomeron. Assuming the prescription for the pomeron flux in the model of Donnachie and Landshoff (DL) [1], different possible parton densities were tested against the data. Shown in figure 5 are the predictions based on a "hard" quark parton density ($zq(z) = \frac{6}{4}z(1-z)$ for two flavours only), a "hard" gluon density ($zg(z) = 6z(1-z)$) and a "soft" gluon density ($zg(z) = 6(1-z)^5$) where in each case any scale dependence of these parton densities is neglected. It is observed that for this particular choice of flux, the data are best reproduced by the hard gluon parameterisation, while both the soft gluon and hard quark parameterisations produce too few jets.

A parameter $\Sigma_{I\!P}$, is defined, equal to the "momentum sum" of the pomeron such that $\Sigma_{I\!P} = \int_0^1 \mathrm{d}z \sum_i f^{DL}_{i/I\!P}(z_i)$ where the sum i is over all of the partons in the pomeron assuming the DL flux. Since the absolute normalisation of the pomeron flux is unknown to any factor N [14], then the relationship between $\Sigma_{I\!P}$ and any momentum sum rule for the $I\!P$ is ill–defined. Assuming that the gluon and quark densities in the pomeron are "hard" (see above), and that a fraction c_g of the momentum of the pomeron is carried by gluons, then the measurement of inclusive jet cross section in photoproduction places a constraint on $\Sigma_{I\!P}$ for a particular value of c_g.

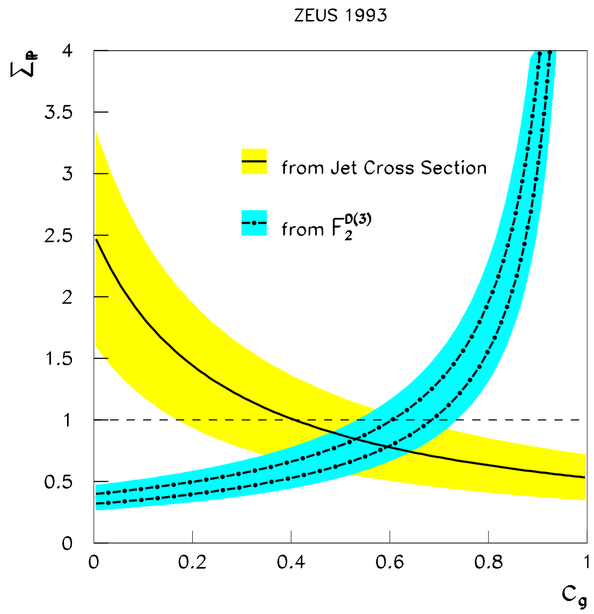

Figure 6. The constrains on the momentum fraction of the pomeron carried by hard gluons. The solid line shows the constraint from the ZEUS measurement of the $d\sigma/d\eta_{jet}(\eta_{max} < 1.8)$. The upper (lower) dot–dashed line shows the constraint from the measurement of $F_2^D(3)$ assuming three (two) quark flavours. The shaded regions represent 1σ of uncertainty.

If the same flux parameterisation (DL) is adopted for deep–inelastic scattering then (in LO) the integral $\int_0^1 \tilde{F}_2^D(\beta, Q^2)\mathrm{d}\beta$ constrains the contribution of quarks to the "momentum sum" $\Sigma_{I\!P}$. The constraints from the measurement of $d\sigma/d\eta_{jet}(\eta_{max} < 1.8)$ and $F_2^D(3)$ are shown in figure 6. The extrapolation of $\tilde{F}_2^D(\beta, Q^2)$ outside of the measure range ($0.175 \leq \beta \leq 0.65$) is done using a parameterisation of the form $\tilde{F}_2^D(\beta, Q^2) = a \cdot \beta(1-\beta) + b \cdot (1-\beta)^2$ [3]. A careful evaluation of the experimental systematic uncertainties associated with the combination of these two constraints leads to the conclusion that $0.3 < c_g < 0.8$ [13]. This combined constraint is independent of the choice of flux and existence of a momentum sum rule, provided that the diffractive cross section is identically factorisable in the deep–inelastic and photoproduction regimes.

5. Comparisons with a Partonic Model of Diffraction

An attempt has been made by Buchmüller and Hebecker [17] to develop a partonic model of diffraction with the assumption that the underlying partonic process is electron–gluon scattering. The motivation is derived from the importance of such dynamics in low–x deep–inelastic ep scattering, and by implication therefore it requires diffractive exchange to be predominantly a leading gluon phenomenon. It is hypothesised that the quark–antiquark pair produced in the hard electron–gluon interaction undergoes colour rotation so that the colour quantum numbers of the initial quark–antiquark system become completely decorrelated from the initial state. Then the probabilities of obtaining a colour singlet or octet configuration in the final state are simply $\frac{1}{9}$ and $\frac{8}{9}$ respectively. This leads to the prediction that diffraction should account for $\sim 1/9$, or $\sim 11\%$ of the proton structure function.

H1 have made a measurement of the total proton elastic diffractive contribution to the proton structure function, $F_2^D(x, Q^2)$ which is related to $F_2^{D(3)}$according to

$$F_2^D(x, Q^2) = \int_x^{0.05} F_2^{D(3)}(x, Q^2, x_{I\!P})\mathrm{d}x_{I\!P}. \qquad (11)$$

This measurement is shown along with a H1 measurement of the proton structure function in figure 7. The ratio $r^D = F_2^D(x, Q^2)/F_2(x, Q^2)$ (also shown) is everywhere $\sim 10\%$, which is compatible with the prediction of Buchmüller et el.

A simple scaling law of the form

$$\xi \; F_2^{D(3)}(\beta, Q^2, x_{I\!P} = \xi)\Big|_{Q^2} = 0.04 F_2(x = \xi, Q^2)\Big|_{Q^2} \qquad (12)$$

is predicted which should hold for any β to the extent that the model predicts little β dependence of $F_2^{D(3)}$. This factor corresponds to the proportion overall of deep–inelastic diffraction being $\frac{1}{9}$. This expectation is confronted by the ZEUS data in figure 8 in which the measurements of $F_2^{D(3)}$for different β are included together with the measurements of $\frac{F_2(x)}{x}$ scaled by a factor 0.04.

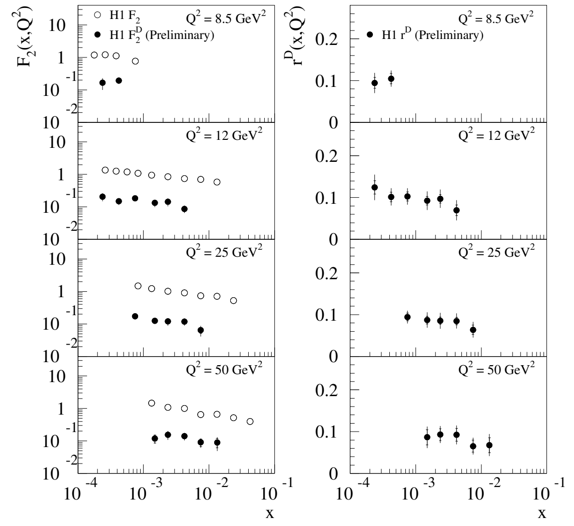

Figure 7. The structure functions $F_2^D(x,Q^2)$ and $F_2(x,Q^2)$, and the ratio $r^D = F_2^D/F_2$ for $x_{I\!P} < 0.05$. The measurement of F_2^D is for proton elastic diffraction.

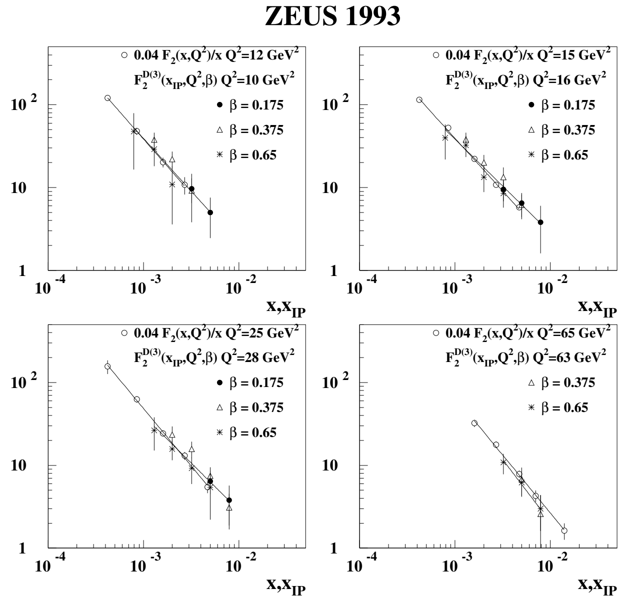

Figure 8. A comparison of $F_2^{D(3)}$ and F_2 to test directly the scaling law prediction of Buchmüller et al. (see text).

The approach of Buchmüller and Hebecker [17] is thus in remarkable agreement with experiment, given the simplicity of the first model calculation in this approach. It adds weight to the picture in which diffractive exchange is a leading gluon phenomenon.

6. Conclusions

The first measurements of $F_2^{D(3)}$, the contribution of large rapidity gap events to the proton structure function, are consistent with a factorisable, diffractive interpretation. A QCD analysis of the dependence of this structure function on Q^2 and on β, the appropriate Bjorken–x like variable, demonstrates consistency with a partonic interpretation, with a potentially large fraction of the diffractive interactions attributable to gluon induced processes. Measurements of jet production in diffractive photoproduction events provide evidence that a significant fraction of the momentum of the diffractive exchange, the pomeron, is carried by gluons.

Acknowledgements

It is a pleasure to thank my colleagues in the H1 and ZEUS collaborations for providing such a wealth of new data in this rapidly evolving field. I would like to thank the conveners of the diffractive session for inviting me to make this presentation. I am particularly indebted to one of the conveners, H. Jung, for his constant enthusiasm throughout the time that I have enjoyed the privilege of working with him. I am grateful to I. MacLeod for making this workshop especially enjoyable.

[1] A. Donnachie, P. V. Landshoff, Phys. Lett. **296** (1992) 227.

[2] T. Ahmed et al. (H1 Collaboration), Phys. Lett. **B348** (1995) 681.

[3] M. Derrick et al. (ZEUS Collaboration), "Measurement of the diffractive structure function in deep inelastic scattering at HERA", DESY preprint DESY 95-093.

[4] H. Jung, Comp. Phys. Commun. **86** (1995) 147.

[5] G. Ingelman and K. Prytz, Z. Phys. **C58** (1993) 285.

[6] H. Jung, *Diffractive Interactions*, these proceedings.

[7] L. N. Lipatov, Sov. Phys. JETP **63** (1986) 904.

[8] É. A. Kuraev, L. N. Lipatov, and V. S. Fadin, Sov. Phys. JETP **45** (1977) 199
Ya. Ya. Balitskiĭ and L. N. Lipatov, Sov. J. Nucl. Phys. **28** (1978) 822.

[9] M. Genovese, N. N. Nikolaev, B. G. Zakharov, "Diffractive DIS from the generalised BFKL pomeron. Predictions for HERA.", Institut für Kernphysik, KFA, Jülich preprint KFA–IKP(Th)–1994–37.

[10] T. Ahmed et al. (H1 Collaboration), "The Gluon Density of the Proton at Low x from a QCD Analysis of F_2", DESY preprint DESY 95–081 (1995).

[11] T. Ahmed et al. (H1 Collaboration), Nucl. Phys. **B435** (1995)3.

[12] M. Derrick et al. (ZEUS Collaboration), Phys. Lett. **B346** (1995) 399.

[13] M. Derrick et al. (ZEUS Collaboration), "Diffractive Hard Photoproduction at HERA and Evidence for the Gluon Content of the Pomeron", DESY preprint DESY 95–115 (1995).

[14] P. V. Landshoff, *Introduction to the pomeron structure function*, these proceedings.

[15] H. G. Bengtsson and T. Sjöstrand, Comp. Phys. Comm. **46** (1987) 43.

[16] P. Bruni and G. Ingelman, Proc. of the International Europhysics Conference, edited by J. Carr and M. Perrotet, Marseille, France, July 1993 (Ed. Frontieres, Gif-sur-Yvette, 1994, p. 595)

[17] W. Buchmüller, A. Hebecker, "A Parton Model for Diffractive Processes in Deep–Inelastic Scattering", DESY preprint DESY 95–077 (1995).